

# A systematic screen of $\beta_2$ -microglobulin and insulin for amyloid-like segments

Magdalena I. Ivanova, Michael J. Thompson, and David Eisenberg\*

Howard Hughes Medical Institute and University of California—Department of Energy Institute of Genomics and Proteomics, University of California, Los Angeles, CA 90095

Contributed by David Eisenberg, December 30, 2005

**Identifying sequence determinants of fibril-forming proteins is crucial for understanding the processes causing >20 proteins to form pathological amyloid depositions. Our approach to identifying which sequences form amyloid-like fibrils is to screen the amyloid-forming proteins human insulin and  $\beta_2$ -microglobulin for segments that form fibrils. Our screen is of 60 sequentially overlapping peptides, 59 being six residues in length and 1 being five residues, covering every noncysteine-containing segment in these two proteins. Each peptide was characterized as amyloid-like or nonfibril-forming. Amyloid-like peptides formed fibrils visible in electron micrographs or needle-like microcrystals showing a cross- $\beta$  diffraction pattern. Eight of the 60 peptides (three from insulin and five from  $\beta_2$ -microglobulin) were identified as amyloid-like. The results of the screen were used to assess the computational method, and good agreement between prediction and experiments was found. This agreement suggests that the pair-of-sheets, zipper spine model on which the computational method is based is at least approximately correct for the structure of the fibrils and suggests the nature of the sequence signal for formation of amyloid-like fibrils.**

fibrils | structure

Amyloid fibrils may be defined as elongated, unbranched protein fibrils that accumulate in the extracellular space of various tissues in connection with disease and that bind Congo red (CR) with characteristic birefringence (1). For example, the intact globular proteins (2) lysozyme and  $\beta_2$ -microglobulin ( $\beta_2m$ ) are deposited as amyloid in hereditary systemic amyloidosis and dialysis-related amyloidosis, whereas type II diabetes is associated with the peptide known as islet amyloid polypeptide (3) and injection amyloidosis with deposits of insulin (4). Human insulin and  $\beta_2m$  are two of the smaller amyloid-forming proteins, and here we have searched systematically for hexameric segments of these proteins that form fibrils or related needle-like microcrystals in isolation from the rest of the protein.

The premise of our work is that small segments of proteins are capable of forming amyloid-like fibrils. In fact, there are numerous examples of small peptides (5–9), some as short as three or four residues, that form fibrils (10, 11). How such short peptides can form fibrils was illuminated by the crystal structures of the amyloid-like peptides of sequence NNQQNY and GNQQNY (12). That study found that the protofibril is built from a pair of  $\beta$ -sheets, whose side chains intermesh at a dry “steric zipper.” That is, the protofibril is an elongated pair of  $\beta$ -sheets, with the  $\beta$ -strands running perpendicular to the fibril axis. Thus a fibril-forming segment need be only as long as the  $\beta$ -sheet is wide.

Amyloid-forming proteins are not in general homologs of each other, and in fact it has been challenging to find any strong sequence signal for the formation of amyloid-like fibrils. Short peptides offer the opportunity for systematic investigation of the sequence determinants of fibril formation, as in the work of Lopez de la Paz and Serrano (6), who varied residues at each position of a known hexameric fibril-forming peptide. Here, we take an alternative strategy of studying which hexameric peptides from the amyloid-forming proteins human insulin

[INS\_HUMAN (P01308) and  $\beta_2m$  (B2MG\_HUMAN (P61769))] themselves form fibrils. These hexamers, which cover all non-cysteine residues of these two proteins, are varied in sequence (see Table 2, which is published as supporting information on the PNAS web site). Because some of these segments are fibril-forming and many others are not, our study is consistent with the idea that there is a strong sequence signature for fibril formation. By comparing our experimental observations to predictions with the 3D profile algorithm of ref. 13, we are able to draw conclusions about the nature of this sequence signature.

## Results

**Definition of Amyloid-Like.** We characterized peptide hexamers by EM, the binding of CR and thioflavin T (ThT), and x-ray diffraction. We consider hexamers to be amyloid-like only if they form straight, unbranched fibrils, 5–15 nm in diameter, or if they form needle-like microcrystals (Fig. 1 D and F) that display the characteristic cross- $\beta$  diffraction pattern (see Fig. 3, which is published as supporting information on the PNAS web site). Although we characterized every peptide by colorimetric and fluorimetric assays with CR or ThT (Table 3, which is published as supporting information on the PNAS web site), the correlation of these assays with the visible formation of fibrils and microcrystals was not high. Also the correlation of predictions from the 3D profile method with these assays was not as strong as with fibril and crystal formation. For these reasons, we do not discuss the detailed results of our colorimetric and fluorimetric assays.

**Solution Conditions for the Screen.** Because both insulin and  $\beta_2m$  form fibrils at low pH (14, 15), we chose pH 2.5 for the fibril formation screen. Fibril formation of both insulin and  $\beta_2m$  is affected by the ionic strength and type of the salt present (14, 16). Insulin usually forms fibrils at low ionic strength (16).  $\beta_2m$  fibril formation requires salt concentrations >100 mM (14). To have uniform conditions for the fibril screen, we chose to use 150 mM NaCl consistent with physiological conditions.

**Systematic Survey of Amyloid Formation with Hexameric Segments from Insulin and  $\beta_2m$ .** The one pentameric and 16 hexameric peptides from the insulin sequence and the 43 hexameric peptides from the  $\beta_2m$  sequence were dissolved and inspected for fibrils or microcrystals (see Table 3). Three of the peptides from insulin and five of the peptides from  $\beta_2m$  form fibrils or elongated microcrystals and qualify as amyloid-like by the definition of this article (Fig. 1 and Table 1).

Of the three amyloid-like peptides from insulin, two (IB11:LVEALY and IB12:VEALYL) are overlapping peptides from the B chain. They are found in the native structure (Fig. 2) in an  $\alpha$ -helix between the two intermolecular disulfide bonds (A7–B7 and A20–B19) and are predicted as fibril formers by the 3D profile

Conflict of interest statement: No conflicts declared.

Abbreviations:  $\beta_2m$ ,  $\beta_2$ -microglobulin; ThT, thioflavin T; CR, Congo red.

\*To whom correspondence should be addressed. E-mail: david@mbi.ucla.edu.

© 2006 by The National Academy of Sciences of the USA

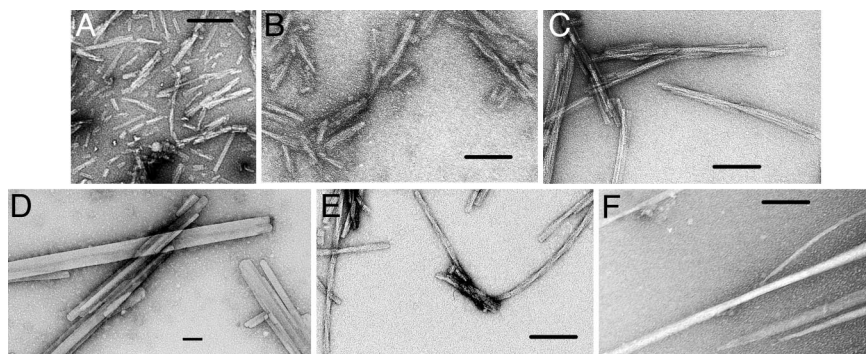


**Fig. 1.** Electron micrographs showing fibrils (A–C and E) and needle-shaped microcrystals (D and F) formed by insulin and  $\beta_2m$  and hexameric peptides from their sequences. (A)  $\beta_2m91$ :KIVKWD. (B)  $\beta_2m83$ :NHVTLT. (C) Full-length  $\beta_2m$ . (D)  $\beta_2m62$ :FYLLYY. (E) Full-length insulin. (F) IB12:VEALYL. The number following the protein name is the position in the protein sequence of the first residue. The sequence of the hexameric peptide follows. The length of the calibration bars is 100 nm.

algorithm. The third amyloid-like peptide from insulin has the sequence IA13:LYQLEN and resides in an  $\alpha$ -helix on the A chain in the structure, also between the two intermolecular disulfide bonds. This peptide is not predicted to form fibrils with the standard energy threshold of  $-21$  kcal/mol we adopt here, but is predicted to form fibrils with the more permissive threshold of  $-19$  kcal/mol. Two other insulin peptides (IA12:SLYQLE and IA14:YQLENY) predicted to form fibrils at the threshold of  $-21$  kcal/mol overlap with IA13:LYQLEN. In fact the nine-residue peptide (A12–A20) that spans all three of these six-residue peptides forms fibrils (data not shown). We conclude that there is good, but not perfect,

agreement between predictions of fibril formation by the 3D profile method and our observations of fibril or needle formation. The extent of agreement mapped onto the 3D protein structures is shown in Fig. 2.

Table 1 also shows that of the eight hexameric peptides from  $\beta_2m$  predicted to be amyloid-like five were found to form fibrils or needle-shaped microcrystals. Earlier we found that fibrils and needle-shaped microcrystals grow under similar solution conditions and have similar structures (12). Also one of the four peptides predicted to form fibrils ( $\beta_2m54$ :LSFSKD) but failing to do so overlaps with a peptide ( $\beta_2m58$ :KDWSFY) that does

**Table 1. The 18 six-residue peptides from insulin (I) and  $\beta_2m$  predicted by the 3D profile method to form fibrils**

Protein, hexamer first residue, and sequence	Amyloid-like fibrils or needles*	X-ray diffraction characterization	Comment <sup>‡</sup>
IA12: SLYQLE			A 9-residue peptide spanning residues A12 to A20 forms fibrils
IA13: LYQLEN	Needles	Needle-like crystals grew in sample buffer <sup>†</sup> and gave cross- $\beta$ pattern	Predicted at threshold $-19$ kcal/mol
IA14: YQLENY			A 9-residue peptide spanning residues A12 to A20 forms fibrils
IB1: FVNQHL			
IB8: GSHLVE			
IB9: SHLVEA			Overlaps needle-forming IB11, IB12
IB10: HLVEAL			Overlaps needle-forming IB11, IB12
IB11: LVEALY	Needles	Needle-like crystals not characterized by x-ray diffraction	
IB12: VEALYL	Long fibrils and needles	Needle-like crystals grew in sample buffer <sup>†</sup> and gave cross- $\beta$ pattern	A 9-residue peptide spanning residues B11 to B19 forms fibrils
$\beta_2m26$ : YVSGFH			
$\beta_2m48$ : KVEHSD			
$\beta_2m52$ : SDLSFS			
$\beta_2m54$ : LSFSKD			Overlaps fibril-forming $\beta_2m58$
$\beta_2m58$ : KDWSFY	Short/medium fibrils	Needle-like crystals grew in conditions C7 and C11 and gave cross- $\beta$ pattern	A 13-residue peptide spanning $\beta_2m$ residues 59–71 forms fibrils (18)
$\beta_2m62$ : FYLLYY	Needles	Needle-like crystals grew in sample buffer <sup>†</sup> and gave cross- $\beta$ pattern	
$\beta_2m64$ : LLYYTE	Needles	Needle-like crystals grew in sample buffer <sup>†</sup> and gave cross- $\beta$ pattern	Predicted at threshold $-19$ kcal/mol
$\beta_2m83$ : NHVTLT	Short fibrils	Needle-like crystals grew in condition E8 and gave cross- $\beta$ pattern	
$\beta_2m91$ : KIVKWD	Short fibrils	Needle-like crystals grew in conditions B11, C5, and E10 and gave cross- $\beta$ pattern	

\*As observed by electron microscopy. Short, medium, and long indicate short, medium, and long amyloid-like fibrils (as shown in Fig. 1 A, B, and E). Needles indicates needle-like crystals (as shown in Fig. 1 D and F).

<sup>†</sup>Sample buffer used for polymerization assays was 150 mM NaCl/50 mM phosphate, pH 2.5.

<sup>‡</sup>Notice that two of the needles were predicted only with the permissive threshold of  $-19$  kcal/mol rather than the standard threshold of  $-21$  kcal/mol.



quence dependence of fibril formation is determined by constraints imposed by the pair-of-sheets, steric zipper structure seen in the structure of GNNQQNY (12). The reason is that the predictions are made by assuming that each hexamer assumes the pair-of-sheets structure, or a structure with minor variations from it, as represented in the ensemble of templates. Table 1 shows neither massive overprediction nor underprediction of observed fibril-forming segments. There are five predicted peptide segments in Table 1 for which no overlapping fibrils or needle-like microcrystals were observed. One of these ( $\beta_2$ m48:KVEHSD) is highly charged, which may offer problems for our energy-based algorithm. There are also two segments whose energies qualify as amyloid formers only at the permissive threshold but not the standard threshold. In practice, someone predicting fibril formation would note the possibility of fibril formation at the permissive threshold. On the whole, the level of agreement between prediction and experiment suggests that the underlying structural model of a pair-of-sheets structure with a dry steric zipper is at least moderately correct for these fibrils.

In short, the sequence signature for formation of amyloid-like fibrils appears to be a short, self-complementary sequence that is compatible with the dry steric zipper interface. The three residues of a hexamer that point into the interface are most important in achieving this self-complementarity. Charged, inward-pointing residues at positions 3 and 5 in the hexapeptide would be expected to be rare, because charged residues would be stacked close to one another, leading to electrostatic destabilization. Charged residues at position 1 are relatively solvent-exposed, particularly if the two  $\beta$ -sheets are shifted out of register with one another in the direction of the  $\beta$ -strands. Consistent with this finding, Lopez de la Paz and Serrano (6) found that the first position of their sequence pattern is tolerant of residue type. Inward-pointing residues greatly differing in size, such as Gly and Trp, would be unlikely, because of the difficulty in achieving a tight, self-complementary interface. Low-complexity sequences, having residues of similar size, might be expected to be favored in fibril-forming sequences, such as NNOQQNY.

## Methods

**Polymerization Assays.** The 60 peptides listed in Table 2 (synthesized by Celtek Bioscience Peptides, Nashville, TN) were dissolved into 1 ml of sample buffer containing 150 mM NaCl/50 mM phosphate, pH 2.5 to a final concentration of 2 mM. Then this 1 ml was split into three and incubated at 37°C with shaking. All measurements (CR and ThT binding) were done immediately after dissolving the peptide, 10–12 and 40–45 days.

**CR Binding Assay.** Spectroscopic assays, detecting a red shift upon binding of CR with peptides, were done as described by Klunk

*et al.* (21). In short, a 5- $\mu$ l sample was added to 75  $\mu$ l of 15  $\mu$ M filtered CR/150 mM NaCl/25 mM phosphate, pH 7.4. The contribution of the scatter was measured by adding a 5- $\mu$ l sample to 75  $\mu$ l of 150 mM NaCl/25 mM phosphate, pH 7.4. The CR alone was measured by adding a 5- $\mu$ l sample buffer to 75  $\mu$ l of 15  $\mu$ M filtered CR/150 mM NaCl/25 mM phosphate, pH 7.4. All specimens were incubated at 37°C for 30 min before signal measurements, which were done at 407, 497, 540, and 550 nm.

**ThT Binding Assay.** A 20- $\mu$ l sample was added to 200  $\mu$ l of 5  $\mu$ M ThT/10 mM Tris, pH 8.0. Emission at 482 nm (2-nm slit width) was measured immediately with excitation at 444 nm (2-nm slit width) by using a Spex Fluorolog spectrofluorimeter (Jobin Yvan, Edison, NJ). Signal was corrected for scatter by subtracting the scatter at 482 nm (20- $\mu$ l sample added to 200  $\mu$ l of 10 mM Tris, pH 8.0) from the signal measured at 482 nm from the sample in ThT.

**EM.** Sample was applied directly to hydrophilic 400-mesh carbon-coated formvar support films mounted on copper grids (Ted Pella, Inc., Redding, CA), allowed to adhere for 4 min, rinsed with distilled water, and stained for 1 min with 1% uranyl acetate (Ted Pella, Inc.). Grids were examined in a Hitachi (Tokyo) H-7000 electron microscope at an accelerating voltage of 75 kV.

**X-Ray Diffraction from Fibrils.** Several hexamers that formed fibrils also formed needle-like crystals after screening with Index HT (HR2-134, Hampton Research, Riverside, CA).

As shown in Table 1, needle-like crystals grew in the following conditions: Index HT screen, B11, 2.1 M DL-Malic acid, pH 7.0, C5 60% (vol/vol) Tacsimate, pH 7.0; C7, 0.8 M KNa Tartrate tetrahydrate/0.1 M Tris, pH 8.5/0.5% (wt/vol) polyethylene glycol monomethyl ether 5000; C11, 1.0 M ammonium sulfate/0.1 M Hepes, pH 7.0/0.5% PEG 8000; E10, 0.1 M Bis-Tris, pH 6.5, 45% (vol/vol) PEG P 400; and Crystal Screen HT, E8, 1.5 M NaCl/10% (vol/vol) ethanol.

Clusters of needle-like crystals of hexamers were transferred to a 2- $\mu$ l drop containing 30% glycerol. Then samples were exposed to copper K $\alpha$  X-radiation from a Rigaku FR-D x-ray generator supplemented with Rigaku Blue Optics operating at 50 kV and 100 mA. Data were collected at 105 K for 5 min with 1° oscillations on a Rigaku IV++ imaging plate detector. X-ray photos were also taken on Beamline ID13 at the European Synchrotron Radiation Facility, Grenoble, France.

We thank Mari Gingery, Michael R. Sawaya, and Martin Phillips for advice on experiments and Melanie J. Bennett for discussion. This work was supported by the National Science Foundation, National Institutes of Health, and the Howard Hughes Medical Institute.

1. Westermarck, P. (2005) *FEBS J.* **272**, 5942–5949.
2. Westermarck, P., Benson, M. D., Buxbaum, J. N., Cohen, A. S., Frangione, B., Ikeda, S., Masters, C. L., Merlini, G., Saraiva, M. J. & Sipe, J. D. (2002) *Amyloid* **9**, 197–200.
3. Westermarck, P., Wernstedt, C., Wilander, E., Hayden, D. W., O'Brien, T. D. & Johnson, K. H. (1987) *Proc. Natl. Acad. Sci. USA* **84**, 3881–3885.
4. Dische, F. E., Wernstedt, C., Westermarck, G. T., Westermarck, P., Pepys, M. B., Rennie, J. A., Gilbey, S. G. & Watkins, P. J. (1988) *Diabetologia* **31**, 158–161.
5. Balbirnie, M., Grothe, R. & Eisenberg, D. S. (2001) *Proc. Natl. Acad. Sci. USA* **98**, 2375–2380.
6. Lopez de la Paz, M. & Serrano, L. (2004) *Proc. Natl. Acad. Sci. USA* **101**, 87–92.
7. Tenidis, K., Waldner, M., Bernhagen, J., Fischle, W., Bergmann, M., Weber, M., Merkle, M. L., Voelter, W., Brunner, H. & Kapurniotu, A. (2000) *J. Mol. Biol.* **295**, 1055–1071.
8. MacPhee, C. E. & Dobson, C. M. (2000) *J. Mol. Biol.* **297**, 1203–1215.
9. Ventura, S., Zurdo, J., Narayanan, S., Parreno, M., Mangues, R., Reif, B., Chiti, F., Giannoni, E., Dobson, C. M., Aviles, F. X. & Serrano, L. (2004) *Proc. Natl. Acad. Sci. USA* **101**, 7258–7263.
10. Reches, M., Porat, Y. & Gazit, E. (2002) *J. Biol. Chem.* **277**, 35475–35480.
11. Tjernberg, L., Hosia, W., Bark, N., Thyberg, J. & Johansson, J. (2002) *J. Biol. Chem.* **277**, 43243–43246.
12. Nelson, R., Sawaya, M. R., Balbirnie, M., Madsen, A. O., Riekel, C., Grothe, R. & Eisenberg, D. (2005) *Nature* **435**, 773–778.
13. Thompson, M. J., Sievers, S. A., Karanicolas, J., Ivanova, M. I., Baker, D. & Eisenberg, D. (2006) *Proc. Natl. Acad. Sci. USA* **103**, 4074–4078.
14. McParland, V. J., Kad, N. M., Kalverda, A. P., Brown, A., Kirwin-Jones, P., Hunter, M. G., Sunde, M. & Radford, S. E. (2000) *Biochemistry* **39**, 8735–8746.
15. Brange, J., Andersen, L., Laursen, E. D., Meyn, G. & Rasmussen, E. (1997) *J. Pharm. Sci.* **86**, 517–525.
16. Whittingham, J. L., Scott, D. J., Chance, K., Wilson, A., Finch, J., Brange, J. & Dodson, G. (2002) *J. Mol. Biol.* **318**, 479–490.
17. Kozhukh, G. V., Hagihara, Y., Kawakami, T., Hasegawa, K., Naiki, H. & Goto, Y. (2002) *J. Biol. Chem.* **277**, 1310–1315.
18. Jones, S., Manning, J., Kad, N. M. & Radford, S. E. (2003) *J. Mol. Biol.* **325**, 249–257.
19. Ivanova, M. I., Gingery, M., Whitson, L. J. & Eisenberg, D. (2003) *Biochemistry* **42**, 13536–13540.
20. Dobson, C. M. (2001) *Philos. Trans. R. Soc. London B* **356**, 133–145.
21. Klunk, W. E., Pettegrew, J. W. & Abraham, D. J. (1989) *J. Histochem. Cytochem.* **37**, 1273–1281.